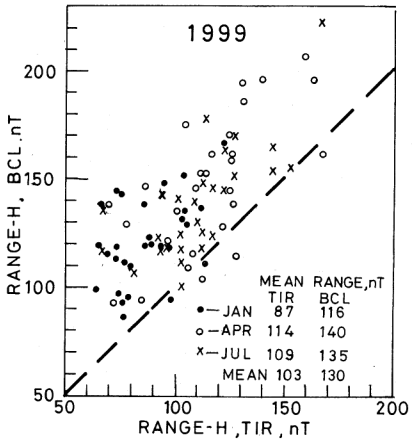

Figure 3. Mass plot of daily range of H field at BCL against the corresponding value at TIR during January, April and July 1999.

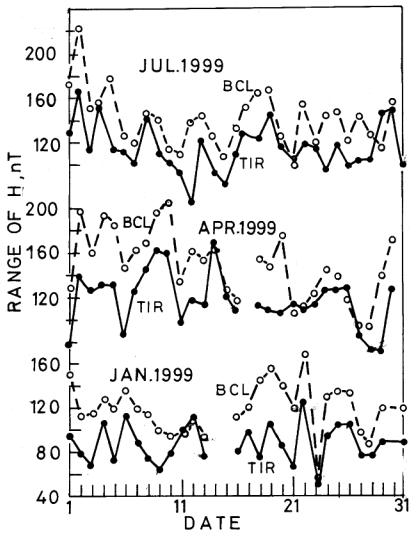

Figure 4. Day-to-day variations of the daily range of H field at BCL and TIR during January, April and July 1999.

and July 1999. These SqH field variations are shown in Figure 2. The daily range of SqH is seen to be clearly larger at BCL than at TIR during any of the months considered. The daily peak occurring about 2 h earlier in universal time further at BCL compared to that at TIR is due to the difference in time at local noon in the two places.

Figure 3 shows the mass plots of the range of H at BCL against the corresponding value at TIR, during the three months of 1999. It is seen that the mean Sq range H values are significantly larger at BCL than at TIR during any of the months. The yearly value is 103 nT for TIR and 130 nT for BCL, indicating an increase of about 27% at BCL over the same at TIR.

Figure 4 is a plot of the individual day value of range of TIR and BCL during the three months of 1999. The value of range H at BCL on any day is larger than that at TIR.

These are descriptions of the variation of the strength of electrojet current at two nearby stations. The present results negate the theory that the ionospheric conductivity over the magnetic equator is inversely proportional to the mean magnetic field.

The day-to-day fluctuations in the range of H being coherent at two stations separated by only 28° in longitude, suggest a longer domain of the electrojet current variations. The source of the electrojet current variations has a much larger extent in space than assumed so far.

It is suggested that the observed variations of EEJ current at different longitudes or on different days are due to corresponding variations of the ionospheric electric fields generated by the local variations in the tidal movements of the upper atmosphere or due to transmission of magnetospheric electric fields.

It is recommended that a more detailed study of ΔH at stations organized by the Kyusha University together with those from permanent geomagnetic observatories could lead to new useful information on the strength, direction and sources of fluctuations of the EEJ current.

1. Chapman, S., *Arch. Meteorol. Geophys. Bioklimatol. Ser. A*, 1951, **4**, 368–390.
2. Rastogi, R. G., *J. Atmos. Terr. Phys.*, 1962, **24**, 1031–1049.
3. Chandra, H., Sinha, H. S. S. and Rastogi, R. G., *Earth Planet Space*, 2000, **52**, 111.

ACKNOWLEDGEMENTS. I thank the Indian Institute of Geomagnetism, Mumbai and Prof. K. Yumoto, Kyushu University, Japan for the data used in the study. Thanks are also due to Physical Research Laboratory, Ahmedabad for facilities and Indian Space Research Organization, Bangalore for the grant of a project on the electrojet monograph.

Received 18 November 2005; revised accepted 31 March 2006

R. G. RASTOGI

Physical Research Laboratory,
Ahmedabad 380 009, India
e-mail: profrgrastogi@yahoo.com

Sulphur isotope composition of galena from Bandalamottu area, Guntur district, Andhra Pradesh

The Agnigundala base metal belt (16°05′–16°20′N lat. and 79°35′–79°50′N long.), traced over a cumulative strike length of about 6 km, is located near Vinukonda, Guntur district in the northeastern part of the Cuddapah Basin (Figure 1 *a*) and constitutes one of the prominent base metal deposits in India. About thirty copper–lead–zinc occurrences are localized within this belt, with Bandalamottu, Nallakonda and Dhukonda constituting the main deposits[1]. Though Cuddapah Basin contains vast resources of mineral wealth, isotopic studies on mineralization are scanty, except for the S-isotopic study of the Mangampeta baryte deposit[2] and Pb, Sr and Nd isotopic studies of uranium-mineralized stromatolitic Vempally dolomites[3]. Variation in isotopic composition of sulphides has an important bearing on type of mineralization. We present here S-isotopic data on carbonate-hosted lead mineralization of the Bandalamottu area, Guntur district, Andhra Pradesh and discuss the role of sulphur in the process of Pb-mineralization.

The Bandalamottu lead deposit (16°14′: 79°43′) is potentially the largest in the Agnigundala poly-sulphide deposit (Ziauddin Mohd. and R. K. Sharma, unpublished). The zones of mineralization are confined mainly to the upper dolostone and dolomitic limestone, which crop out

along the southern flank of the Bandalamottu hill, striking ENE-WSW and dipping 20–35° WNW (Figure 1 *b*) (Y. G. K. Murthy *et al.*, unpublished). The dolostone bed is the thickest in the middle and thins down on either end. It is interbedded with cherty dolostone, sandstone and calcareous sandstone, belonging to the Cumbum Formation of Nallamalai Group of the Cuddapah Supergroup. A detailed account on the geology and mineralization of the area has been given earlier[4–9]. Achaeans, represented by the metamorphic biotite–schists and amphibolites, are the oldest rocks in this area. In addition, granites and dolerite dykes are also found. The Bairankonda Formation, represented by grey, fine-grained, hard and compact sandstones with intercalated shale/slate units, except at a few places, directly overlies the granitic basement. The Cumbum Formation is an argillaceous unit comprising shale, slaty-shale, slate and phyllite interbedded with fine-to-medium and coarse sandstone, and dolostone/dolomitic limestone at various levels. The Pb–Zn mineralized dolostone is rather restricted in occurrence as beds of varying thickness within the chlorite phyllite. The formations are folded, faulted and highly disturbed. Ore mineralization is concordant to bedding, though, in detail it occurs as lodes composed of veins, fracture-fillings and disseminations. Galena is the main mineral with subordinate sphalarite, chalcopyrite and pyrite. Apart from Pb, Ag, Zn, Cu and Cd are obtained as co-products from this area[10].

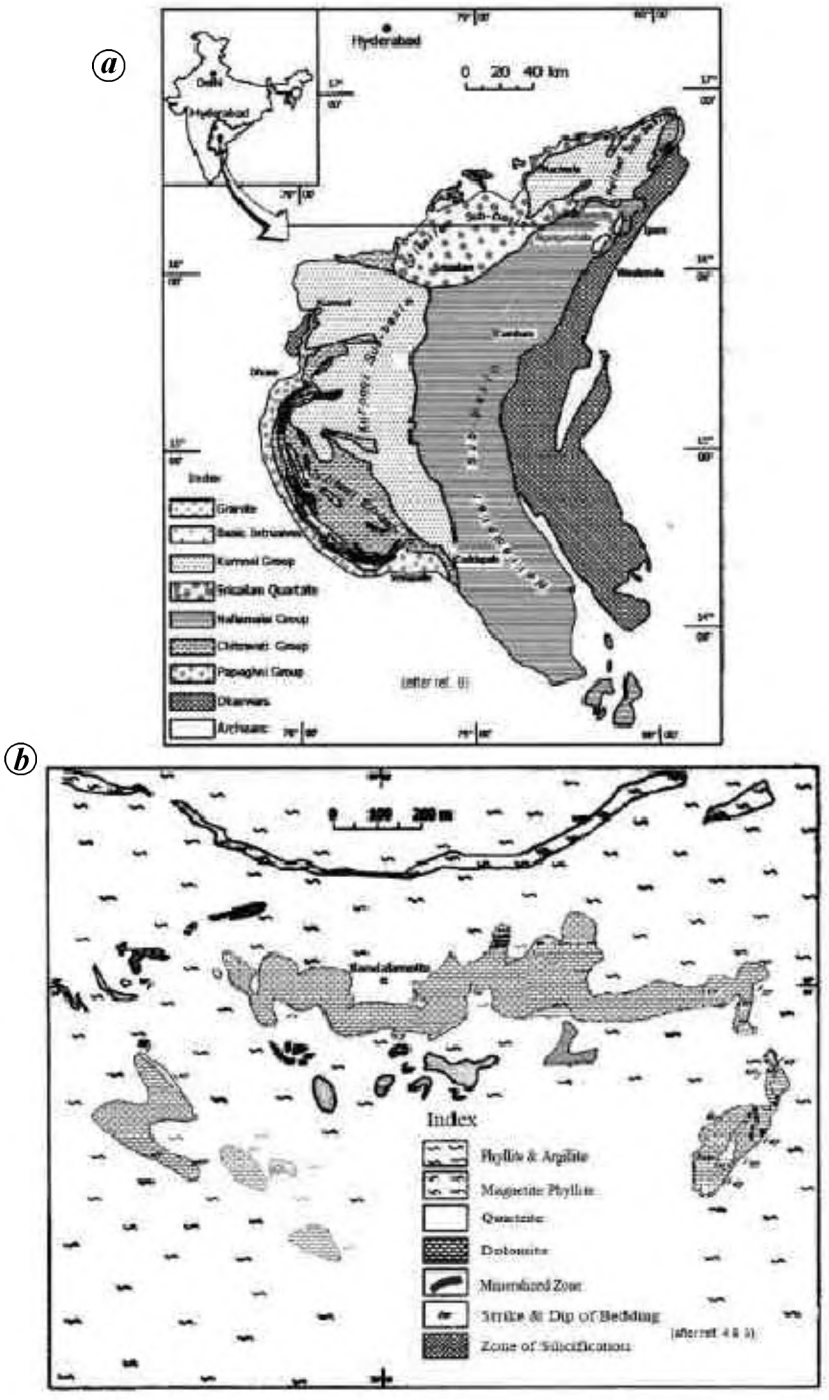

Figure 1. *a*, Location map of Bandalamottu deposit in Cuddapah Basin. *b*, Geological map of the Bandalamottu area.

The dolostone is fine-grained, hard, compact, and grey to cream-coloured on freshly broken surfaces and brown coloured on weathered surface. Occurrence of calcite and quartz, in the form of veinlets, veins, stringers, lenses and as discontinuous discordant bodies, is observed. Chert commonly occurs as nodules, thin beds and irregular replacement bodies. The dolostone comprises equidimensional mosaic of dolospar, as the major phase, followed by minor quartz and calcite. Chert and argillaceous matter are major constituents in some rocks. The texture is granoblastic represented by medium to coarsely crystalline mosaic and many of the dolomite crystals are subhedral to euhedral, exhibiting the idiotopic fabric of Friedman[11]. The mineralized dolostone has intermittent segregation of galena, with its associated sulphides in the form of disseminations, veins, stringers and breccia-fillings.

Coarse crystal aggregate of galena visible to the naked eye was separated using a dentist's micro-drill[12] and fine-grained galena was separated by crushing galena-rich portions of the samples. The galena-bearing fractions, obtained by both the methods, were powdered to –120 # size and subjected to heavy-mineral separation using bromoform and methylene iodide to remove the gangue minerals like quartz, dolomite, sericite, etc. From the heavy-mineral fraction, magnetite was removed with the help of a hand magnet, and then the fraction was subjected to magnetic (isodynamic) separation at 0.8 A to separate chalcopyrite and at 1.2 A to separate other sulphide minerals, if present. The fraction was then subjected to hand-pick-

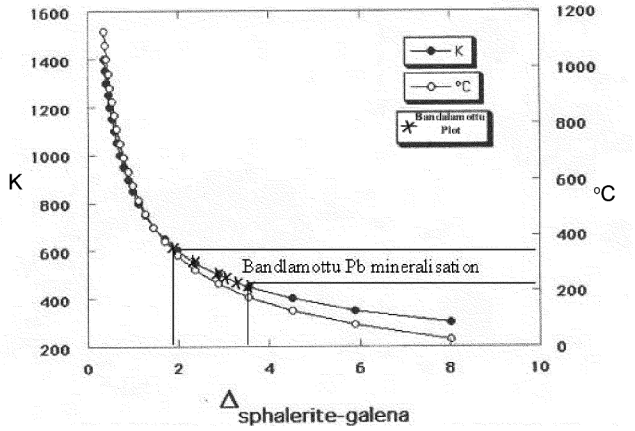

Figure 2. Bandalamottu mineralization range through isotope data.

Table 1. S-isotopic data (in ‰) on dolostone-hosted galena of the Bandalamottu area, Andhra Pradesh

Sample no	$\delta^{34}S$ CDÒ
AL/BM/1	+3.3
AL/BM/2	+3.3
AL/BM/7F	+3.0
AL/BM/8	+2.8
AL/BM/9	+3.5
AL/BM/9F	+2.8
AL/BM/16	+1.8
AL/BM/19	+2.2

ing under a binocular microscope to remove impurities from the pure fraction. Final fraction of galena thus obtained is of ~ 99% purity. Sulphur isotope analysis of pure fractions of separated galena was carried out on a double-collector electron bombardment (gaseous source) mass spectrometer, VG 602D. Mass spectrometric measurement was carried out to determine the ratio of two stable isotopes of sulphur (^{34}S and ^{32}S). Standard used for comparison and calculation is troilite of the Canyon Diablo iron Meteorite (CDT)[13], with $^{34}S/^{32}S$ ratio of 0.0450045.

About 50 mg of galena was taken for analysis. The galena sample was first mixed with copper oxide and oxidized in a combustion tube under vacuum at about 900°C. The released SO_2 gas was collected using liquid nitrogen trap and the non-condensable gases were pumped-off. It was further purified by first removing moisture using a liquid nitrogen–chlorobenzene trap at – 40°C and then transferred to liquid nitrogen–*n*-pentane trap at –130°C to condense SO_2 and pump-off traces of CO_2. The SO_2, thus purified was collected in the collection finger using liquid nitrogen trap. The preparation and purification line of SO_2 used is similar to that described by Fritz *et al.*[14]. The $^{34}S/^{32}S$ ratio was determined according to the method described by Ahmad *et al.*[15], employing 'VG 602 D micromass' mass-spectrometer. Final values are reported with respect to CDT standard. The standard deviation of mass spectrometric measurement is ± 0.05‰. The overall reproducibility is ± 0.5‰.

The S-isotopic data obtained on eight galena samples, expressed as $\delta^{34}S$ with respect to CDT-standard as per mil (‰), are given in Table 1.

The $\delta^{34}S$ values obtained are all positive and show a narrow spread between + 1.8 and 3.5‰, with an average of 2.8‰ CDT. Generally, such a tight grouping of $\delta^{34}S$ values indicates uniform source of sulphur for galena. Intrusions with mantle-derived sulphur typically have isotopic compositions near 0‰ and associated deposits commonly contain sulphur[16], ranging from + 5 to –5‰. The ratio obtained in the present study corresponds to the published values of $\delta^{34}S$ of magmatic/hydrothermal origin[17]. This range of values rules out the biogenic or terrestrial extra-basinal source of sulphur and indicates that the dominant component of this sulphur was from deep-seated magmatic source. The discharge of ore fluids from the hydrothermal vents on the basin floor and their reduction with interaction of sea water has possibly led to the formation of ore minerals. Thus, the values possibly indicate magmatic origin for sulphur in the galena samples under study. The restricted range of $\delta^{34}S$ of galena is comparable with that of sulphide minerals of the Rangpo deposit having similar positive $\delta^{34}S$ values[18], with a narrow spread between + 2.61‰ and +6.57‰. This is corroborated by the field and petromineralogical aspects like vein and disseminated type of mineralization of galena as well as the possible genetic link between the mineralization and closeby domal structures, formed due to emplacement of granitic magma. However, the isotope ratio of the samples when plotted against the temperature dependance of the galena–sphalerite fraction (Figure 2)[20] indicates that the temperature of fractionation varies from 225 to 375°C, suggesting hydrothermal origin for the galena in the area.

S-isotopic study on galena from the Bandalamottu area shows a restricted range that is characteristic of magmatic–hydrothermal-type deposits. It appears that the source of sulphur for this deposit has a predominant hydrothermal component of the granitic magma, which had evolved by chemical reduction of seawater in a hydrothermal system, and was carried towards the seafloor with other leached metals.

1. Ramam, P. K., *Mineral Resources of Andhra Pradesh*, Geological Society of India, Bangalore, 1999, pp. 176–183.
2. Neelakantam, S., Memoirs Geological Society of India, Bangalore, 1987, vol. 6, pp. 429–458.
3. Zachariah, J. K., Bhaskar Rao, Y. J., Srinivasan, R. and Gopalan, K., *Chem. Geol.*, 1999, **162**, 49–64.
4. King, W., *Geol. Surv. India, Mem.*, 1872, vol. 8, pp. 269–270.
5. Ziauddin, Md., *J. Indian Geol. Sci. Assoc.*, 1964, **4**, 107–111.
6. Dutt, N. V. B. S., *Geology and Mineral Resources of Andhra Pradesh*, Ramesh Publications, Hyderabad, 1975, pp. 1–205.
7. Ramana Rao, N. and Reddy, M. N., *Indian Mineral.*, 1976, **17**, 39–48.
8. Nagaraja Rao, B. K., Rajurkar, S. T., Ramalinga Swamy, G. and Ravindhra Babu, B., *Mem. Geol. Soc. India*, 1987, **6**, 33–86.
9. Kale, V. S., *Constraints on the Evolution of the Purana Basins of Peninsular India*, Geological Society India, 1991, vol. 38, pp. 231–252.
10. Sivadas, K. M. *et al.*, *Geol. Surv. India, Mem.*, 1985, **118**, 1–101.
11. Friedman, G. M., *J. Sediment. Petrol.*, 1965, **35**, 643–665.
12. Hutchison, C. S., *Laboratory Handbook of Petrographic Techniques*, John Wiley, New York, 1973, p. 113.
13. Ault, W. V. and Jensen, M. L., In *Biogeochemistry of Sulfur Isotopes* (ed. Jensen, M. L.), Natl. Sci. Found. Symp. Proc., Yale University, 1963.
14. Fritz, P., Drimmie, R. J. and Nourcki, V. N., *Anal. Chem.*, 1974, **46**, 164–166.

15. Ahmad, M. A., Rajendra Singh, Diwakara Singh and Prasad, R. N., In Third Natl. Symp. on Mass Spectrometry – Research, Applications and Instrumentation, Regional Research Laboratory, Hyderabad, 1985, pp. 12/1–12/2.
16. Sangster, D. F., In *Geol. Assoc. Can. Proc.*, 1968, vol. 19, pp. 79–91.
17. Mason, B. and Moore, C. B., *Principles of Geochemistry*, John Wiley, New York, 1982, pp. 1–344.
18. Rai, K. L. and Madhusudana Rao, In *Recent Researches in Geology*, Wadia Institute of Himalayan Geology, 1993, vol. 14, pp. 67–79.
19. Sirish Chander, T., *J. Geol. Min. Metall. Soc. India*, 1979, **51**, 149–154.
20. http://www.huxley.ic.ac.uk/local/earthSciUG/ESFirstYR/EarthMaterials/mrpalmer/Earth.

ACKNOWLEDGEMENTS. We thank Shri R. M. Sinha, Director, Atomic Minerals Directorate for Exploration and Research (AMD), Department of Atomic Energy, Hyderabad for encouragement and laboratory support. We thank B. K. Pandey, D. D. Pandey and K. Asha, Geochronology Lab, AMD for providing valuable data during laboratory investigations and Dr V. Divakar Rao, former scientist, NGRI for critically going through the manuscript. Finally we thank the anonymous referee whose comments helped improve the quality of the paper.

Received 7 December 2005; revised accepted 18 March 2006

R. PAVANAGURU[1,*]
ASOORI LATHA[2]

[1]*Department of Geology, Osmania University, Hyderabad 500 007, India*
[2]*Atomic Minerals Directorate for Exploration and Research, Hyderabad 500 016, India*
**For correspondence.*
e-mail: pavanaguru@rediffmail.com

Entropy as an indicator of fragmented landscape

Human-induced fragmentation in forest landscape involves the substitution of contiguous natural land covers by any natural, semi-natural or anthropogenic types, resulting in disconnected and isolated patches of nature[1]. In simple terms, patches consist of communities surrounded by a matrix with a dissimilar community structure or composition[2]. Fragmentation leads to habitat loss, isolation and edge effects[3,4] and subsequent degradation of ecosystem. It is considered to have the largest impact of all drivers on biodiversity change[5]. The main cause behind this increase is biotic impact in an area.

Fragmentation itself is a matrix easily agreed upon to understand the landscape. It is obvious that fragmentation over a space could be represented using geospatial tools[6]. The problem however is to introduce a quantitative measure of forest fragmentation. An adequate fragmentation matrix is consequently needed for policy development with respect to nature and biodiversity conservation. Developing this analogy, the mathematical representation of degradation and the concept of entropy are close (entropy was often used as a measure of degradation). In this way, information theory can offer an appropriate framework to approach the landscape as a spatial information system[7]. Moreover, it is demonstrated that heterogeneity (pattern) and entropy can be considered as equivalent terms[8]. In the present study, entropy is used as a measure of the fragmentation process, i.e. a measure of disorderness in the forest patches. In order to develop this concept and to demonstrate its applicability to a natural ecosystem, we used Shannon's entropy index to quantify the intrusion of non-forest to forest area (conversion of forest patches into non-forest areas). Analysis of cartographic data or remote sensing imagery to analyse the pattern heterogeneity (entropy) of an entire landscape implies data completeness: the complete landscape or image pattern is always analysed (often using a Geographic Information System (GIS))[8], and is not estimated by use of a sample or subset of the landscape of interest.

The study area, Northeast India, extends from 88–97°E and 22–29°30′N, with a geographical area of about 255,083 km^2. The area consists of 25% of the total forest cover of the country. The altitude in the study area varies from the low-lying plains of Brahmaputra to around 6000 m in parts of Arunachal Pradesh. The climate varies from typical tropical to sub-alpine. Since last three decades, the area is being affected by intense land-cover changes. The land use practices consist of activities for timber collection, shifting cultivation, mining, permanent agriculture, etc. The practice of shifting cultivation has been found to be the major cause behind forest fragmentation. It results into conversion of dense forests to open forests as well as non-forests including shifting cultivation. About 0.45 million families in the northeastern region annually cultivate 10,000 km^2 of the forests, whereas total area affected by 'jhuming' (shifting cultivation)[9] is about 44,000 km^2. With the phenomenal increase in human population, the 'jhum' cycle has been decreased from 20 to 30 years in the past to about 3–5 years in many areas. Reduction in the 'jhum' cycle due to increase in pressure on land because of population increase has accelerated the process of land degradation, which has further enhanced eco-degradation[10]. Earlier workers have reported a high degree of forest fragmentation in this landscape[6,11–13].

We analysed four historical datasets to relate entropy to the degree of forest fragmentation over a multi-decadal period forest cover estimate of Forest Survey of India (FSI) for the years 1987 (ref. 14), 1989 (ref. 15), 1993 (ref. 16) and 2001 (ref. 17). For maps showing the pattern dynamics of Northeast India, the forest cover and its relation with population has been carried out. The contiguous vegetation in the entire Northeast is fragmented due to shifting cultivation and other forest extraction processes[18]. The dense forest cover has decreased with increase in population. It reflects the impact of biotic factors on forest areas. After 1989, there is stability in dense forest cover, while population has increased with almost the same rate. The rate of decrease in dense forest was slow between the years 1987 and 1993, and dense forest cover increased during the years 1993 and 2001. This is due to regeneration in abandoned shifting cultivation areas and density improvement[17,19]. Also, change in forest policies and interim ban imposed